Our Dermatology Online

Original Article

Total Actinic Keratosis Burden Score (TABS) and Field Index: A Dermoscopy-Based Framework for Quantifying Actinic Field Damage

Gökhan Kaya

Department of Dermatology, Sivas Medicana Hospital, Sivas, Türkiye

Corresponding author: Gökhan Kaya, MD, E-mail: gkhnkya@gmail.com

ABSTRACT

Background: Actinic keratosis (AK) encompasses both clinically apparent lesions and extensive subclinical photodamage. Traditional lesion-centric assessment methods inadequately reflect total actinic burden, thus limiting accurate risk stratification and treatment planning. **Objective:** To develop and validate a dermoscopy-based scoring framework—the Total Actinic Keratosis Burden Score (TABS) and Field Index (FI)—to comprehensively quantify lesion severity and subclinical field damage in AK patients. **Methods:** In this retrospective-prospective study, dermoscopic images of 200 participants (100 AK patients, 100 controls) were systematically evaluated using structured criteria to determine lesion scores, field scores, TABS (0–36), and FI (% field contribution). Clinical and demographic data were analyzed to validate the scoring system. **Results:** AK patients had significantly higher dermoscopic field scores than controls (5.91 ± 1.71 vs. 4.70 ± 1.44; $p < 0.001$). The mean TABS was 16.24 ± 2.86 and the mean FI was 36.2% ± 7.96. TABS correlated moderately with lesion count ($\rho = +0.34$; $p < 0.001$) and age ($\rho = +0.25$; $p = 0.011$), whereas FI was independent of lesion number. Phenotypic stratification showed lesion-dominant (9%), mild field (28%), moderate field (48%), and severe field-dominant (15%) subgroups, confirming that extensive subclinical burden exists even in patients with few visible lesions. **Conclusion:** The TABS–FI system is a concise, quantitative, dermoscopy-guided framework that integrates lesion and field parameters. It enables more accurate risk stratification and supports phenotype-based, personalized therapeutic strategies in AK management.

Key words: Actinic Keratosis, Dermoscopy, Field Cancerization, Scoring System, Tabs; Field Index

INTRODUCTION

Actinic keratoses (AK) are premalignant epidermal lesions caused by chronic ultraviolet radiation (UV) on sun-exposed skin. Risk factors include older age, male sex, Fitzpatrick I–II phototypes, immunosuppression, and photosensitizing drugs such as hydrochlorothiazide. Epidemiological studies also implicate prolonged outdoor activity, light hair/eye color, and facial solar lentigines, while sunscreen use and higher BMI (≥25) offer partial protection [1,2].

A systematic review estimated a global prevalence of ~14%, with regional variation driven by UV exposure, skin type, and healthcare access [3]. Despite this burden, AK is frequently underdiagnosed and inconsistently managed. Lesion-targeted therapies dominate, field-directed approaches remain underused, and referral pathways are often inefficient [4].

Although clinically similar, AKs differ biologically. Confluent, hyperkeratotic "AK patches" carry higher malignant risk, whereas most lesions remain stable or regress. This variability underscores the need for individualized risk stratification [5,6].

The broad morphological spectrum—including flat, pigmented, and atypical forms—complicates diagnosis. Routine biopsies are impractical in patients with extensive damage [7]. Dermoscopy identifies

How to cite this article: Kaya G. Total Actinic Keratosis Burden Score (TABS) and Field Index: A Dermoscopy-Based Framework for Quantifying Actinic Field Damage. Our Dermatol Online. 2026;17(3):289-303.

Submission: 02.02.2026; **Acceptance:** 30.04.2026
DOI: 10.7241/ourd.20263.2

© Our Dermatol Online 3.2026

characteristic features such as red pseudonetworks, perifollicular scaling, and the "strawberry pattern," but limited depth restricts invasion assessment. Advanced non-invasive imaging (RCM, OCT, LC-OCT) provides near-histological resolution, aiding early detection of atypia [8,9].

Field cancerization, described by Slaughter et al. in 1953, denotes perilesional tissue with subclinical genetic change [10]. In AK, chronically sun-exposed skin shows UV-induced atypia and mutations, justifying field-based therapy [11]. Photodamage refers to benign visible changes (solar lentigo, seborrheic keratosis, telangiectasia) [12,13], while actinic field damage encompasses visible and subclinical alterations with malignant potential [14,15]. Photodamage is limited to clinically benign signs [16,17]; actinic field damage represents a continuum including histological or molecular dysplasia, invisible clinically but detectable by dermoscopy, histopathology, or biomarkers [18–20].

Commonly used clinical metrics, such as total lesion count (TLC), Physician Global Assessment (PGA), or composite AK burden scores, fail to reflect the underlying histological severity or subclinical field involvement [21]. Clinical grading systems, including the Olsen scale, correlate poorly with histopathological classification [22]. The Actinic Keratosis Area and Severity Index (AKASI) integrates both lesion burden and field involvement, and higher scores have been associated with an increased risk of progression to cSCC [23,24].

Genomic data show a multistep progression from AK to carcinoma, beginning with TP53 and NOTCH1 mutations, followed by CDKN2A, PIK3CA, FBXW7 alterations and MAPK, NF-κB, PI3K/AKT/mTOR dysregulation [25–27]. Figure 1 summarizes these histological, molecular, and immunologic changes.

Despite multiple therapies, lesion-directed approaches prevail. Cryotherapy, the most common, fails to address subclinical field cancerization and recurs frequently. Field-directed treatments such as PDT, imiquimod, and 5-FU provide broader control; among these, 5-FU shows superior clearance and long-term cSCC risk reduction [28–30].

The combined use of the Total Actinic Keratosis Burden Score (TABS) and the Field Index (FI) provides a quantitative, dermoscopy-based system that captures both lesion and field dimensions, thereby enabling more precise risk stratification and personalized therapeutic planning.

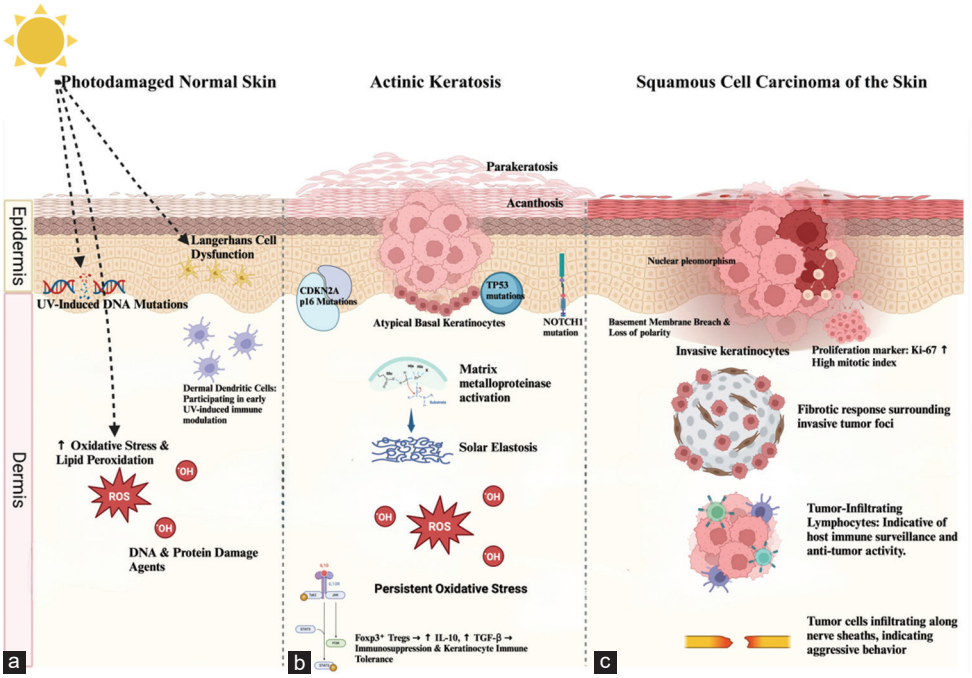

Figure 1: Multistep transformation from photodamaged skin (a) to actinic keratosis (b), culminating in invasive cSCC (c). (a) Chronic UV exposure induces DNA mutations (e.g., C>T, CC>TT), oxidative stress, and immune dysregulation in epidermal and dermal compartments. (b) AK is marked histologically by atypical basal keratinocytes, solar elastosis, and MMP-mediated matrix remodeling. Genomic mutations in TP53 and CDKN2A drive clonal expansion, while regulatory T cell infiltration suppresses anti-tumor immunity. (c) cSCC features full-thickness atypia, Ki-67 overexpression, and perineural invasion, reflecting malignant transformation.

MATERIALS AND METHODS

Study Design and Participants

Data were collected from the Dermatology Department of Nizip State Hospital between May 2024 and May 2025. Adults clinically diagnosed with AK were identified through retrospective reviews of electronic medical records and prospective enrollment during routine dermatology consultations. A total of 200 individuals participated: 100 AK patients and 100 age- and sex-matched controls without AK.

AK patients were identified through multiple recruitment pathways, including individuals presenting with visible facial discoloration or photodamage-related concerns; participants in Euromelanoma public awareness campaigns conducted at the study center [31]; and patients attending dermatology clinics for unrelated conditions who were incidentally diagnosed with AK during full-skin examinations. In addition, residents of affiliated long-term care facilities (nursing homes) were systematically screened during institutional dermatologic visits, enabling the inclusion of older individuals with limited outpatient access. Patients admitted to other hospital departments-such as internal medicine, geriatrics, and neurology—were also evaluated via dermatology consultations when clinically indicated.

All dermoscopic evaluations were performed by a specialist dermatologist. Participants were consecutively enrolled. Exclusion criteria included topical treatment (5-fluorouracil, imiquimod, or photodynamic therapy) within the previous 12 months, due to potential alteration of dermoscopic features.

Clinical and Dermoscopic Assessment

All participants underwent standardized dermatological evaluation. In AK patients, both visible lesions and adjacent perilesional skin were examined, while controls underwent dermoscopic assessment of sun-exposed, lesion-free areas (typically forehead or malar regions). Anatomical sites were systematically documented. Dermoscopy was performed using a polarized handheld dermoscope (DermLite DL5, DermLite Inc., CA, USA) attached to a smartphone camera. Examinations were conducted in polarized mode at ×10 magnification, using contact fluid when required. Prior to imaging, participants were instructed to remove sunscreen, moisturizers, or cosmetics to avoid interference with dermoscopic features. All images were acquired under standardized indoor lighting at a fixed distance, using the same dermoscope–smartphone setup throughout the study to ensure consistency. Between one and three AK lesions and adjacent sun-damaged fields were imaged per patient. All images were stored in a secure, cloud-based, password-protected database accessible only to the study team.

Clinical data-including Fitzpatrick skin type, lesion localization, and occupational background—were obtained from electronic records. Occupational roles were categorized into four groups according to estimated ultraviolet (UV) exposure: (i) outdoor/high exposure (e.g., farming, construction, animal husbandry); (ii) indoor/low exposure (e.g., office work, teaching); (iii) domestic/partially outdoor (e.g., homemaking, small-scale trade); and (iv) retired/other. This classification was used for subgroup analyses and UV stratification.

The diagnosis of AK was supported by dermoscopic criteria. Non-pigmented lesions exhibited features such as erythematous pseudonetworks, keratotic scales, and the classic "strawberry pattern," whereas pigmented variants demonstrated brown pseudonetworks and granular-annular structures. Lesions with suspicion for invasive transformation underwent biopsy, with histopathological confirmation performed in accordance with validated diagnostic algorithms [32,33].

Field Area Selection and Photodamage Spectrum Assessment

Non-lesional skin areas were selected according to the presence of dermoscopic signs of chronic photodamage. Chronically sun-exposed regions (vertex, forehead, malar areas) were preferentially assessed. Dermoscopic features evaluated included solar lentigines, mottled pigmentation, telangiectasia, seborrheic keratoses, yellowish discoloration, superficial and deep wrinkles, diffuse erythema, and reticular pigmentation. Representative dermoscopic examples of these photoaging-related changes are provided in Figure 2 [12,13,34].

Scoring Methodology

A structured dermoscopic scoring system was applied to both clinically visible AK lesions and adjacent sun-damaged field areas. Two components were evaluated: the Lesion Score, representing the severity of visible AKs, and the Field Score, reflecting subclinical

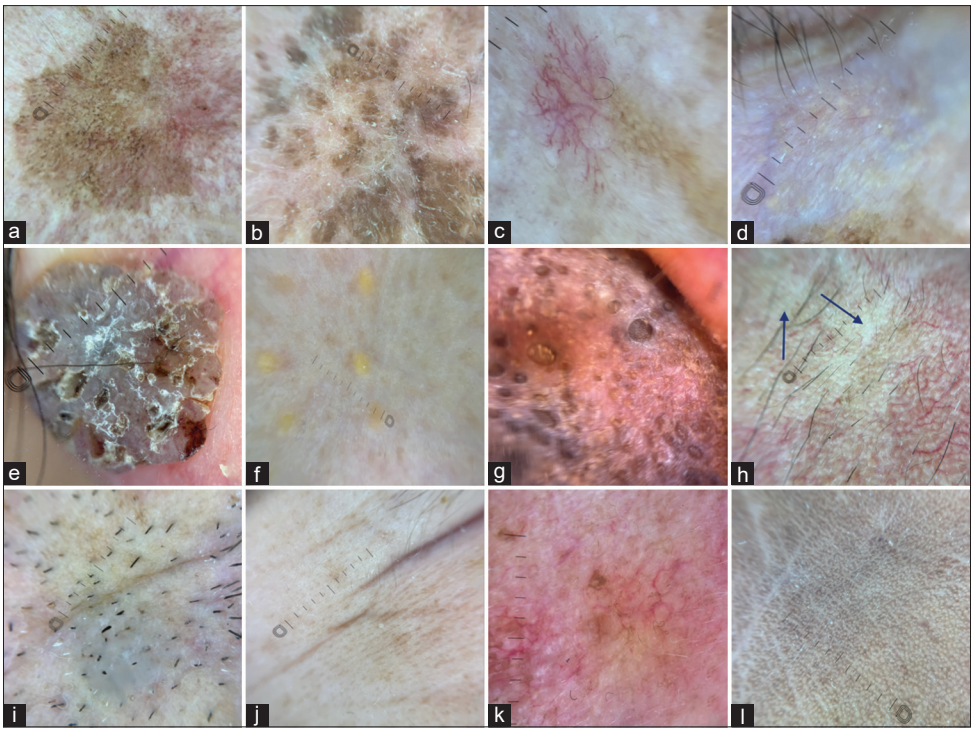

Figure 2: Dermoscopic Spectrum of Photoaging-Related Cutaneous Changes. Representative dermoscopic features of photodamaged skin: (a) Solar lentigo showing a symmetric pigmented pseudonetwork; (b) Mottled pigmentation with irregular light- and dark-brown areas; (c) Telangiectasia with fine linear or branching vessels; (d) Diffuse yellowish discoloration consistent with dermal elastosis; (e) Seborrheic keratosis with comedo-like openings and cerebriform surface; (f) Yellow papules corresponding to elastotic deposits; (g) Senile comedones as follicular keratin plugs; (h) Superficial wrinkles as fine, parallel lines; (i) Deep wrinkles as broad furrows; (j) Criss-cross wrinkles with a grid-like pattern; (k) Diffuse erythema indicating subclinical inflammation; (l) Reticular pigmentation as a brownish reticulated network.

photodamage. Six dermoscopic features (granular structures, scale, follicular keratotic plugs, vascular pattern, background pigmentation, and rosettes) were scored on a 4-point scale (0–3), yielding a maximum of eighteen points per site. When multiple lesions or field areas were present, arithmetic means were calculated. The scoring criteria for both lesions and field areas are summarized in Table 1.

The Total Actinic Keratosis Burden Score (TABS) was defined as the sum of the mean lesion and field scores (range 0–36). The Field Index (FI) quantified the proportional contribution of field involvement to total burden: FI (%) = Field Score ÷ TABS × 100. A phenotype-based stratification matrix using predefined TABS and FI thresholds is provided in Table 2. Conceptual correlations between dermoscopic parameters and histopathology are illustrated in Figure 3, and representative grading examples for each feature (mild → severe) are shown in Figure 4.

Statistical Analysis

Sample size estimation was performed using G*Power (version 3.1.9.7; Universität Düsseldorf, Germany), assuming a medium effect size (Cohen's d = 0.5), $\alpha = 0.05$, and statistical power of 80%, indicating that 200 participants (100 per group) were sufficient.

All analyses were conducted in Python (version 3.8; Python Software Foundation, Wilmington, DE, USA) using the libraries *pandas*, *NumPy*, *SciPy*, and *seaborn*. Descriptive statistics were expressed as mean ± standard deviation (SD) for normally distributed variables, or as median with interquartile range (IQR) for non-normal data. Normality was assessed with the Shapiro–Wilk test.

Between-group comparisons were performed using independent-samples *t*-test (parametric) or Mann–Whitney U test (non-parametric), while categorical variables were compared by chi-square or Fisher's exact tests. Effect sizes (Hedges' *g*) with 95% confidence intervals (CIs) were calculated where appropriate.

Within the AK cohort, associations between continuous variables were evaluated using Spearman's rho. Multivariable linear regression was used to identify independent predictors of TABS. Logistic regression models explored predictors of severe field involvement (FI >45%), and ROC curve analysis was performed for

Table 1: Dermoscopic scoring criteria for AK lesions and sun-damaged field areas

Dermoscopic Feature	0 – None	1 – Mild	2 – Moderate	3 – Severe/Prominent
Granular pattern/structures	Absent	Scattered gray dots	Diffuse perifollicular granules or annular pattern	Dense clusters with widespread annular pattern
Scale	None	Fine, superficial scaling	Diffuse thin scale or focal thickening	Thick keratin plaques/crusts
Follicular keratotic plugs	None	1–2 plugged follicles	3–5 plugs	Numerous/prominent plugs throughout
Vascular pattern/erythema	None	Faint telangiectasias or erythema	Linear or branched vessels	Starburst, polymorphic or glomerular vessels
Background pigmentation	Absent	<10% pigmented	10–50% pigmented	>50% pigmented
Rosettes/white circles	Not observed	1–2 rosettes	3–4 scattered	≥5 or widespread

Six dermoscopic features (granular pattern, scale, follicular keratotic plugs, vascular pattern, background pigmentation, and rosettes) were assessed using a 4-point scale (0–3). Scores were assigned separately for visible AK lesions and adjacent sun-damaged skin, yielding a maximum of 18 points per site. When multiple lesions or field areas were evaluated, mean values were calculated

Table 2: Phenotypic stratification of actinic keratosis using TABS and field index (FI)

TABS Range	FI <25% (Lesion-dominant)	FI 25–35% (Mild field involvement)	FI 35–45% (Moderate field involvement)	FI >45% (Severe field involvement)
0–10 (Low burden)	Minimal disease	Subclinical field AK	—	—
11–17 (Moderate burden)	Focal AK	Early actinic field damage	Field–lesion overlap	Subclinical field-dominant AK
≥18 (High burden)	Multifocal AK	Mixed–mild field	Multifocal field AK	Extensive field cancerization

This matrix outlines a phenotype-based classification of actinic keratosis presentations, integrating lesion and field characteristics into a single framework. By capturing the relative dominance of focal lesions versus background photodamage, it supports nuanced interpretation of actinic burden and guides risk-aligned treatment planning

region count; however, discriminatory performance was poor. All statistical tests were two-tailed, and $p < 0.05$ was considered statistically significant.

Ethical Considerations

The study was conducted in accordance with the Declaration of Helsinki and complied with Good Clinical Practice (GCP) guidelines. Ethical approval was obtained from the Scientific Research Ethics Committee of Bezmialem Vakıf University (Approval No: 2025/184; Official Document No: E-54022451-050.04-194649, dated 24 May 2025). Given the retrospective design and the use of anonymized clinical and dermoscopic data, the requirement for written informed consent was formally waived by the Ethics Committee. No personally identifiable information was collected or stored. All patient data and dermoscopic images were anonymized and securely stored in encrypted, password-protected servers accessible only to the study investigators.

RESULTS

A total of 200 participants were included (100 AK, 100 controls). AK patients were significantly older than controls (70.0 ± 11.1 vs. 64.6 ± 12.7 years; p = 0.0015). Sex distribution did not differ (p = 0.197), while Fitzpatrick phototypes showed significant differences (p < 0.001). Occupational UV exposure categories were comparable (p = 0.758). Dermoscopic field scores were significantly higher in the AK group (5.91 ± 1.71 vs. 4.70 ± 1.44; p < 0.001; Hedges' g = 0.76). Detailed demographic and clinical data are summarized in Table 3.

Figure 5 illustrates sex-based differences in the anatomical distribution of AK lesions. Males most frequently exhibited lesions on the vertex, ears, and frontotemporal region, while females showed higher involvement of the cheeks, infraorbital, and nasal areas.

Among AK patients, the mean Lesion Score was 10.3 ± 2.0 and the mean Field Score was 5.9 ± 1.7, yielding a mean TABS of 16.2 ± 2.9 and an average FI of 36.2% ± 8.0. Based on predefined thresholds, most patients were classified as moderate burden (69%) with moderate field involvement (48%), while 15% showed severe field-dominant phenotypes. Detailed stratification is presented in Table 4.

Regression analyses showed that higher TABS values were significantly associated with older age (p = 0.011), while sex, Fitzpatrick type, and occupational UV exposure showed no consistent effects. Importantly, FI was not correlated with lesion number or region count, underscoring its independence from visible distribution. Patients with TABS ≥18 were significantly older and had higher field scores than those with lower TABS. Subgroup results are detailed in Table 5.

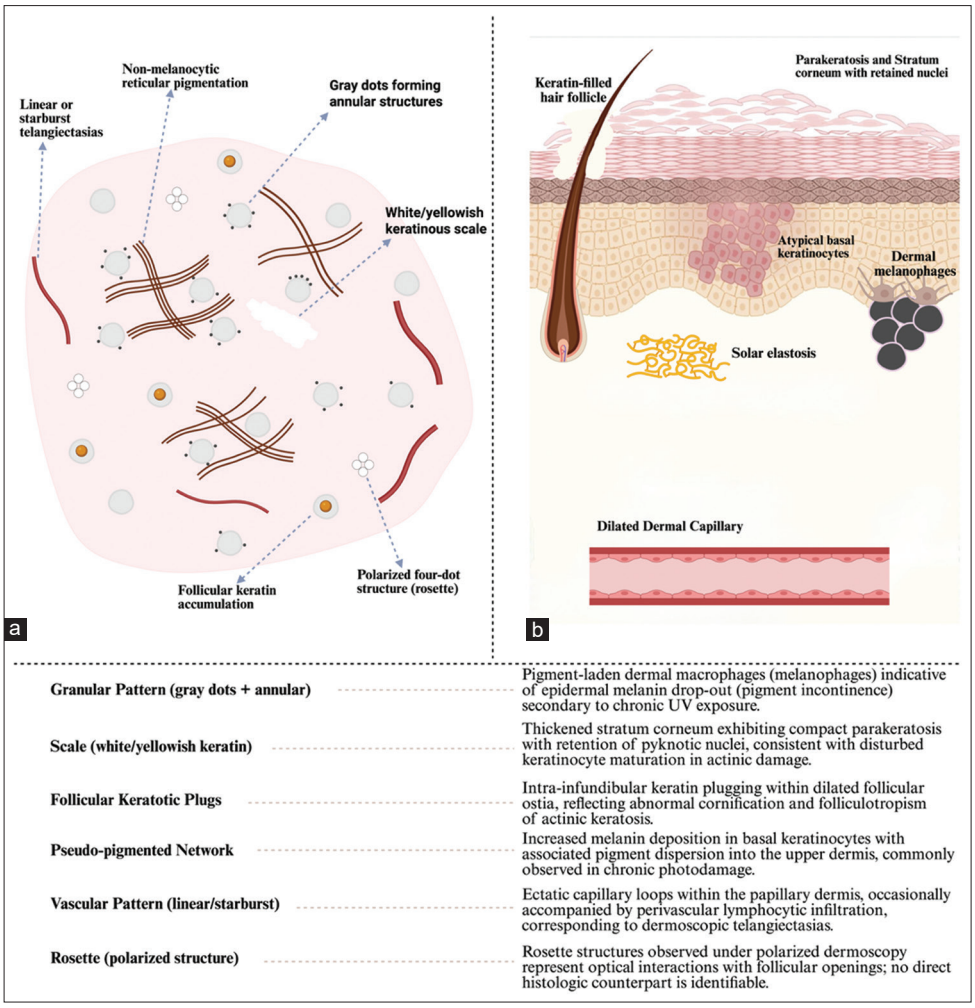
Non-melanocytic reticular pigmentation
Gray dots forming annular structures
Linear or starburst telangiectasias
White/yellowish keratinous scale
Follicular keratin accumulation
Polarized four-dot structure (rosette)
a
Keratin-filled hair follicle
Parakeratosis and Stratum corneum with retained nuclei
Atypical basal keratinocytes
Dermal melanophages
Solar elastosis
Dilated Dermal Capillary
b
Granular Pattern (gray dots + annular)
Pigment-laden dermal macrophages (melanophages) indicative of epidermal melanin drop-out (pigment incontinence) secondary to chronic UV exposure.
Scale (white/yellowish keratin)
Thickened stratum corneum exhibiting compact parakeratosis with retention of pyknotic nuclei, consistent with disturbed keratinocyte maturation in actinic damage.
Follicular Keratotic Plugs
Intra-infundibular keratin plugging within dilated follicular ostia, reflecting abnormal cornification and folliculotropism of actinic keratosis.
Pseudo-pigmented Network
Increased melanin deposition in basal keratinocytes with associated pigment dispersion into the upper dermis, commonly observed in chronic photodamage.
Vascular Pattern (linear/starburst)
Ectatic capillary loops within the papillary dermis, occasionally accompanied by perivascular lymphocytic infiltration, corresponding to dermoscopic telangiectasias.
Rosette (polarized structure)
Rosette structures observed under polarized dermoscopy represent optical interactions with follicular openings; no direct histologic counterpart is identifiable.

Figure 3: Dermoscopic and histopathologic correlation of actinic keratosis based on the TABS scoring system. Panel a schematically illustrates an AK lesion incorporating the six dermoscopic parameters: granular pattern, scale, follicular plugs, pseudo-pigmented network, vascular pattern, and rosettes. Panel b depicts corresponding histopathologic features including parakeratosis, basal keratinocytic atypia, follicular plugging, pigment dispersion, dermal melanophages, dilated capillaries, and solar elastosis. This model highlights how the cumulative severity of dermoscopic findings reflects increasing histological burden, underscoring the clinical relevance of TABS scoring.

Combined analyses confirmed that age, occupational UV exposure, and region count were not significant predictors of severe field involvement (FI >45%). Region count showed poor discriminatory performance (AUC = 0.46). Correlation analysis revealed that lesion count correlated moderately with TABS ($\rho = +0.34$, $p < 0.001$) but not with FI, while age showed only a weak association with TABS ($\rho = +0.25$, $p = 0.011$). Full results are presented in Table 6.

DISCUSSION

This study assessed AK burden using the dermoscopy-based TABS and FI. These complementary tools capture both visible lesion severity and subclinical field damage, offering a more comprehensive assessment than traditional lesion counts. By integrating clinical, dermoscopic, and demographic data, the TABS–FI framework stratified AK patients into phenotypes reflecting the balance between focal lesions and background photodamage. The study included 200 chronically sun-exposed individuals (100 AK patients, 100 age- and sex-matched controls), allowing evaluation of demographic and clinical predictors of disease severity.

In our cohort, patients with AK had a mean age of 70.0 years, significantly higher than that of controls (64.6 years, $p = 0.0015$), confirming age as a key determinant of actinic damage. This observation aligns with epidemiological studies demonstrating a marked rise in AK prevalence with advancing age [35,36]. Although sex distribution did not differ significantly between groups (male/female: 63/37 vs.

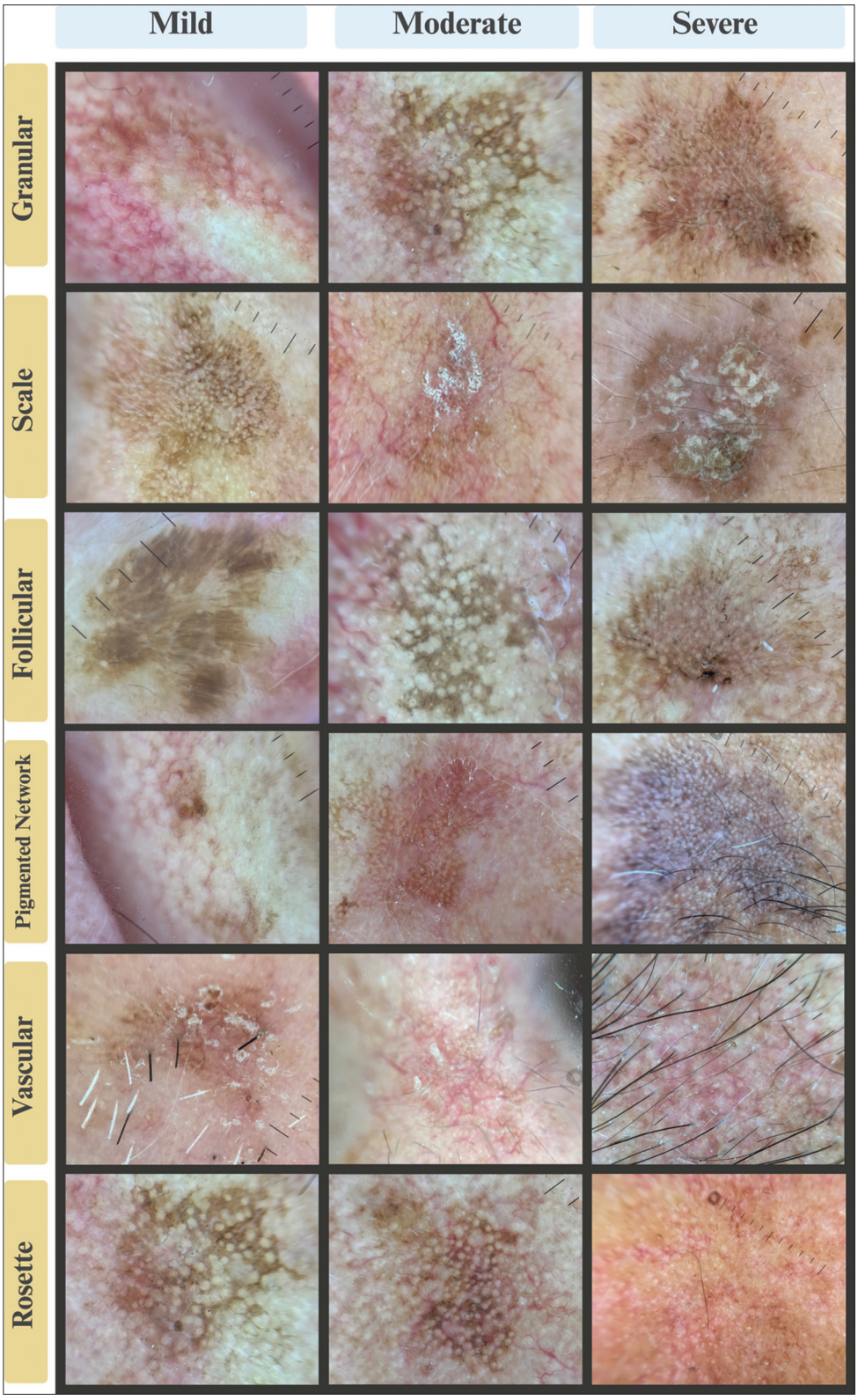

Figure 4: Grading of Dermoscopic Features in Actinic Keratosis. Representative dermoscopic images demonstrating the grading (mild [1], moderate [2], and severe [3]) of six distinct dermoscopic features commonly observed in actinic keratosis: granular pattern, scale, follicular keratotic plugs, pseudo-pigmented network, vascular pattern, and rosette structures. This systematic grading approach facilitates standardized assessment, enhances diagnostic accuracy, assists clinical severity evaluation, and enables precise monitoring of therapeutic response.

53/47, p = 0.197), prior research has consistently shown a male predominance, commonly attributed to androgenic alopecia, greater occupational sun exposure, and less frequent photoprotection [37]. Fitzpatrick

Table 3: Demographic and clinical characteristics of patients in the AK and control groups

Variable	AK Group (n=100)	Control Group (n=100)	*p*-value
Age, years (mean±SD)	70.04±11.13	64.60±12.70	0.0015†
Sex, n (%)	Male 63 (63%) Female 37 (37%)	Male 53 (53%) Female 47 (47%)	0.197‡
Fitzpatrick phototype, n (%)	Type I: 1 (1%) Type II: 35 (35%) Type III: 45 (45%) Type IV: 19 (19%)	Type II: 7 (7%) Type III: 43 (43%) Type IV: 48 (48%) Type V: 2 (2%)	<0.001‡
UV exposure category, n (%)	Low: 14 (14%) Semi-exposed: 32 (32%) High: 53 (53%) Other/Retired: 1 (1%)	Low: 13 (13%) Semi-exposed: 35 (35%) High: 52 (52%) Other/Retired: 0 (0%)	0.758‡
Dermoscopic field score (0–18, mean±SD)	5.91±1.71	4.70±1.44	<0.001†

Demographic variables, skin phototypes, occupational UV exposure categories, and dermoscopic field scores are compared between AK patients and matched controls. Mean age and field scores were significantly higher in the AK group, whereas sex distributions were comparable. Fitzpatrick types differed modestly, while occupational UV categories were similar across groups (*p* values from Chi-square or Welch's *t*-test as appropriate; $p < 0.05$ considered statistically significant).Demographic variables, skin phototypes, occupational UV exposure categories, and dermoscopic field scores are compared between AK patients and matched controls. Mean age and field scores were significantly higher in the AK group, whereas sex distributions were comparable. Fitzpatrick types differed modestly, while occupational UV categories were similar across groups (*p* values from Chi-square or Welch's *t*-test as appropriate; $p < 0.05$ considered statistically significant)

†Welch's t-test.

‡Chi-square test.

$p < 0.05$ considered statistically significant

Table 4: Summary of dermoscopic scores and phenotypic classification in the AK group

Parameter	Value
Lesion Score (0–18), Mean±SD	10.33±2.01
Field Score (0–18), Mean±SD	5.91±1.71
TABS (0–36), Mean±SD	16.24±2.86
Field Index (%), Mean±SD	36.20±7.96
Number of AK lesions, Mean±SD	2.67±2.09
TABS Classification, n (%)	
– Low burden (0–10)	3 (3%)
– Moderate burden (11–17)	69 (69%)
– High burden (≥18)	27 (27%)
FI Classification, n (%)	
– Lesion-dominant (FI <25%)	9 (9%)
– Mild field involvement (FI 25–35%)	28 (28%)
– Moderate field involvement (FI 35–45%)	48 (48%)
– Severe field involvement (FI >45%)	15 (15%)

Mean dermoscopic lesion and field scores are presented along with the calculated Total Actinic Burden Score (TABS) and Field Index (FI). TABS was calculated as the sum of lesion and field scores (range: 0–36), while FI (%) represents the proportional contribution of field damage. Patients were further stratified into burden categories (low, moderate, high) according to TABS and into lesion- or field-dominant phenotypes according to FI thresholds. Values are expressed as mean±SD or n (%)

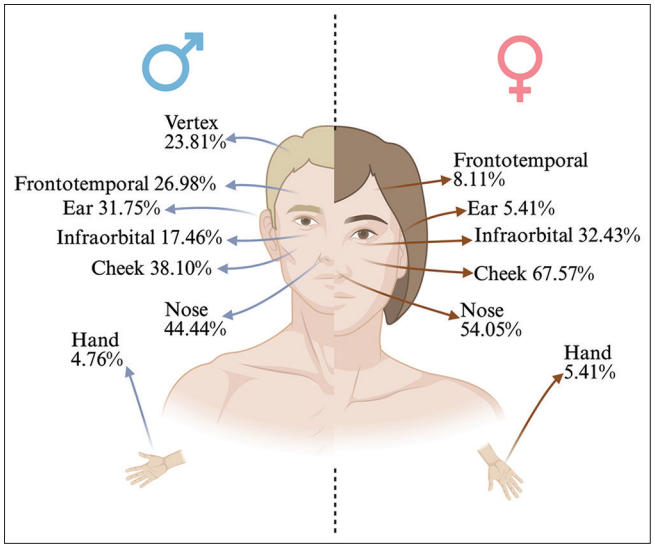

Figure 5: Schematic representation of the anatomical distribution of AK lesions among study participants by sex. This composite illustration highlights sex-based differences in the anatomical distribution of actinic keratosis (AK). In male participants, lesions were most frequently observed on the vertex (23.8%), ears (31.8%), and frontotemporal region (27.0%), followed by the cheeks (38.1%), nose (44.4%), and infraorbital area (17.5%). By contrast, female participants demonstrated predominant involvement of the cheeks (67.6%), infraorbital area (32.4%), and nose (54.1%), with lower prevalence on the frontotemporal (8.1%) and auricular (5.4%) regions. Hand involvement was reported in 4.8% of males and 5.4% of females.

phototypes differed significantly ($p < 0.001$), with AK patients more often displaying lighter skin types, supporting meta-analyses that highlight elevated risk in phototypes I–II [38]. In contrast, occupational UV exposure categories showed no significant differences between groups ($p = 0.758$), diverging from multicenter reports linking high occupational sun exposure with increased AK burden. This discrepancy may reflect limitations of occupational classification or, more importantly, the predominant role of cumulative lifetime UV exposure and inherent skin type in shaping disease risk.

Analysis of lesion distribution showed clear sex-related patterns. In males, AKs were most common on the nose (44.4%), cheeks (38.1%), and ears (31.8%). In females, facial involvement predominated, particularly the cheeks (67.6%) and nose (54.1%). The high prevalence of auricular lesions in men agrees with prior studies,

Table 5: Predictors and stratified differences in actinic burden

Analysis Section	Variable/Subgroup	TABS (mean±SD)	FI (%) (mean±SD)	p-value
Multivariable regression (TABS)	Age	β=+0.25	—	0.011
	UV category	n.s.	—	0.76
	Male sex	n.s.	—	0.74
	Fitzpatrick type	n.s.	—	n.s.
Stratified by UV exposure	Low UV	15.9±2.7	35.4±7.2	0.76
	Semi-exposed	16.3±2.8	37.0±7.5	—
	High UV	16.5±3.0	36.8±7.8	—
Stratified by region count	1–2 anatomical sites	15.8±2.6	36.2±7.5	0.29
	≥3 anatomical sites	16.6±3.1	36.5±7.6	—
TABS stratification (≥18 vs < 18)	Age	72.1±9.8 vs 68.0±11.5	—	0.04
	Field Score	6.9±1.9 vs 5.5±1.6	—	<0.01
	Region Count	2.1±1.0 vs 1.7±0.8	—	0.06

Regression and subgroup analyses demonstrated that higher TABS values were significantly associated with older age (p=0.011), whereas no consistent associations were observed for sex, Fitzpatrick type, or occupational UV exposure. Field Index (FI) values did not correlate with lesion number or region count, indicating that field damage is independent from visible lesion distribution. Patients with TABS ≥ 18 were significantly older and exhibited higher field scores compared to those with lower TABS. Values are expressed as mean±SD, regression coefficients (β), or Spearman's ρ, as appropriate (p < 0.05 considered statistically significant)

Table 6: Unified predictive, comparative, and correlational analysis table

Analysis Type	Variable	Estimate	95% CI/Statistic	p-value
Logistic regression (F >45%)	Age (years)	OR=0.999	0.95 – 1.05	0.982
	UV category	OR=0.80	0.37 – 1.70	0.556
	Region count	OR=0.82	0.41 – 1.66	0.588
ROC analysis (FI >45%)	Region count	AUC=0.46	0.34 – 0.58	0.607
Spearman correlations	Lesion count vs. TABS	ρ = +0.338	—	0.0006
	Lesion count vs. FI	ρ = –0.028	—	0.780
	Age vs. TABS	ρ = +0.254	—	0.011

Logistic regression and ROC curve diagnostics did not identify age, occupational UV exposure, or anatomical region count as significant predictors of severe field involvement (FI >45%), with region count showing poor discriminatory ability (AUC = 0.46). Correlation analyses demonstrated that lesion count was moderately associated with TABS but not with FI, whereas age showed a weak positive correlation with TABS. Values are reported as odds ratios (OR) with 95% confidence intervals, AUC with 95% CI, or Spearman's ρ, as appropriate (p < 0.05 considered statistically significant)

whereas the pronounced female facial predominance—possibly influenced by hair coverage, headwear, or cosmetic photoprotection—contrasts with reports of higher chest and leg involvement in other populations. These population-specific patterns underscore the need for preventive counseling tailored to anatomical sites most affected in each sex [39].

Occupational UV exposure categories did not differ significantly between AK patients and controls ($p = 0.758$). This diverges from multicenter European studies reporting increased AK risk with high occupational sun exposure. As Fartasch et al. highlight, both occupational and non-occupational (e.g., recreational) UV exposure must be considered, with cumulative lifetime dose likely more relevant than job categorization [40]. In our region, indoor workers often engage in secondary agricultural activities, and high ambient sunlight may blur categorical distinctions, explaining the absence of a clear occupational signal. These findings suggest that lifetime cumulative exposure and skin type exert stronger effects than current occupation.

Our findings highlight the clinical utility of the TABS–FI system in quantifying subclinical burden. In our cohort, the FI was diagnostically independent of visible lesion counts ($\rho = -0.028$, $p = 0.780$), confirming that lesion number alone fails to capture background photodamage. This is consistent with clinical trial evidence showing that visible lesion counts underestimate field cancerization, as topical 5-FU unmasks numerous subclinical lesions beyond baseline [41]. Imaging and histopathology likewise demonstrate photodamage extending beyond clinical borders, reinforcing AK as a continuum of visible and subclinical disease [42]. Notably, 15% of our patients exhibited severe field involvement despite few visible lesions, illustrating the 'hidden burden' emphasized in current S3 guidelines [43]. TABS also correlated positively with age ($\rho = +0.254$, $p = 0.011$), validating it as a pragmatic marker of cumulative UV exposure [44].

To enhance specificity, the TABS–FI model excludes benign UV-induced changes such as solar lentigines and seborrheic keratoses and instead focuses on dermoscopic features with premalignant potential. This is particularly relevant

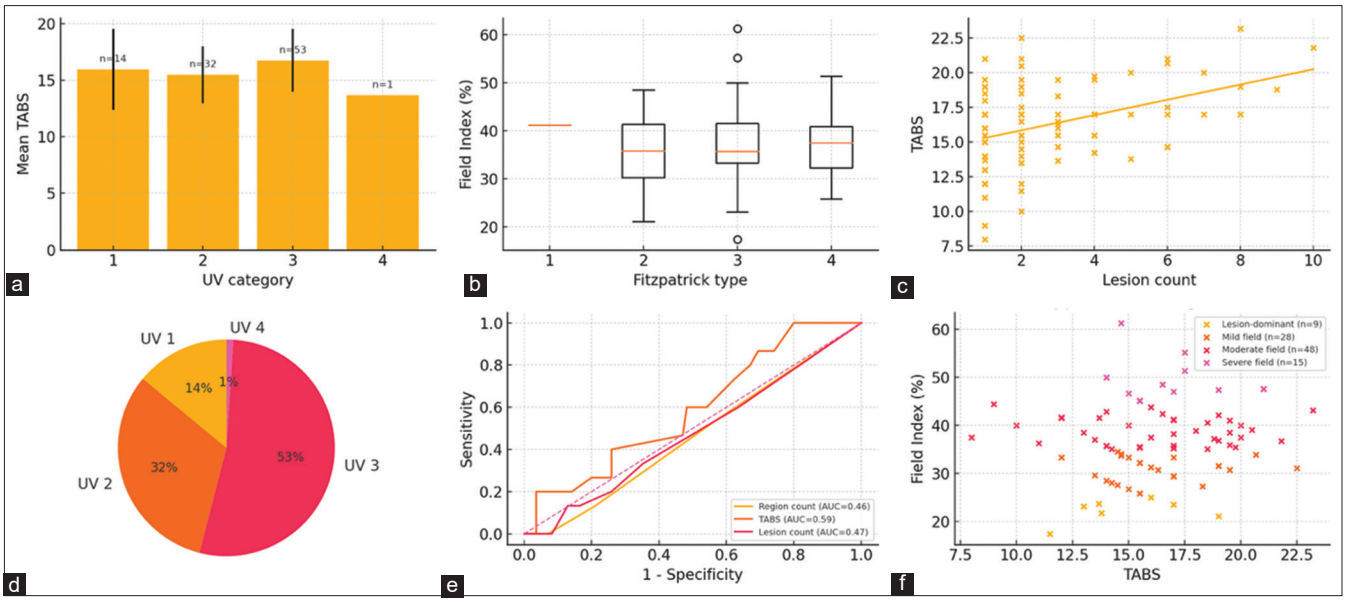

Figure 6: Composite visualization of clinical, dermoscopic, and phenotypic parameters in actinic keratosis. (a) Mean Total Actinic Keratosis Burden Score (TABS) across ultraviolet (UV) exposure categories, with no significant between-group differences. (b) Distribution of Field Index (FI) values across Fitzpatrick phototypes, illustrating inter-type variability in subclinical photodamage. (c) Scatterplot of lesion count versus TABS showing a moderate positive correlation (Spearman's $\rho = 0.36$, $p = 0.0006$). (d) Distribution of occupational UV exposure categories within the AK cohort, with high UV exposure (UV3) representing 53% of patients. (e) Receiver operating characteristic (ROC) curves for severe field involvement (FI > 45%): region count (AUC = 0.46), lesion count (AUC = 0.47), and TABS (AUC = 0.59), indicating poor discriminatory value of conventional variables and only marginal predictive capacity of TABS. (f) Phenotypic clustering based on TABS and FI thresholds, stratifying patients into lesion-dominant (n = 9), mild field (n = 28), moderate field (n = 48), and severe field (n = 15) phenotypes.

Table 7: Comparison of quantitative scoring systems for actinic keratosis evaluation

Scoring System	Components Assessed	Field Component	Lesion Component	Numeric Score	Anatomical Mapping	Dermoscopy-Based	Risk Stratification
AKASI (Dirschka et al., 2017; Pellacani et al., 2018)	Solar damage, erythema, thickness	Incorporated	Included	Quantitative	Fixed regions (head only)	Not integrated	Supported
PGA	Physician-rated global severity (0–4)	Not evaluated	Included (global)	Not numeric	Not applicable	Not integrated	Subjective estimate
TLC (McCampbell et al., 2023)	Total count of AK lesions	Not evaluated	Included	Not applicable	Not applicable	Not integrated	Limited clinical utility
AK-FAS (Dréno et al., 2017)	AK area %, hyperkeratosis, sun damage	Incorporated	Included	Categorical	Not specified	Not integrated	Supported
PAASI (Nevakivi et al., 2024)	Visual photodamage severity by region	Incorporated (field only)	Not evaluated	Quantitative (regional weighting)	Anatomical zone-based	Not integrated	Supported (field burden only)
MASCK (Baker et al., 2022)	AK number + thickness, % area, global score, cancer-in-zone	Incorporated	Included	Quantitative (0–30)	Multiple sites validated	Not integrated	Supported (field severity, reproducible)
Soare et al., 2025 (Experimental)	Clinical, dermoscopic and confocal features (erythema, vessels, microerosions, "strawberry" pattern)	Incorporated	Included	Semi-quantitative (0–3 scale)	Per lesion	Partly integrated	Investigational; not validated for routine risk stratification
TABS + FI (Current study)	6 dermoscopic lesion+6 dermoscopic field criteria	Integrated	Integrated	Quantitative	Flexible anatomical regions	Fully integrated	Quantitative FI-based stratification

AKASI, Actinic Keratosis Area and Severity Index; PGA, Physician Global Assessment; TLC, Total Lesion Count; AK-FAS, Actinic Keratosis Field Assessment Scale; PAASI, Photoaging Area and Severity Index; MASCK, Method for Assessing Skin Cancerization and Keratoses; TABS–FI, Total Actinic Keratosis Burden Score and Field Index This table summarizes the key features of current actinic keratosis scoring frameworks. Conventional indices (AKASI, PGA, TLC, AK-FAS, PAASI, MASCK, and the more recent Soare et al. composite clinical–dermoscopic–confocal approach) each provide partial insights but remain limited by reliance on clinical or photographic features, restricted anatomical scope, or lack of dermoscopic integration. In contrast, the TABS–FI model uniquely integrates lesion- and field-based dermoscopic criteria, offers flexible anatomical mapping, and delivers quantitative FI-based stratification. These attributes enhance clinical utility and support individualized patient management.

in pigmented variants, which may mimic melanoma or lentigo maligna and often require histopathology for confirmation [45,46]. By incorporating multiple lesion- and field-specific dermoscopic parameters,

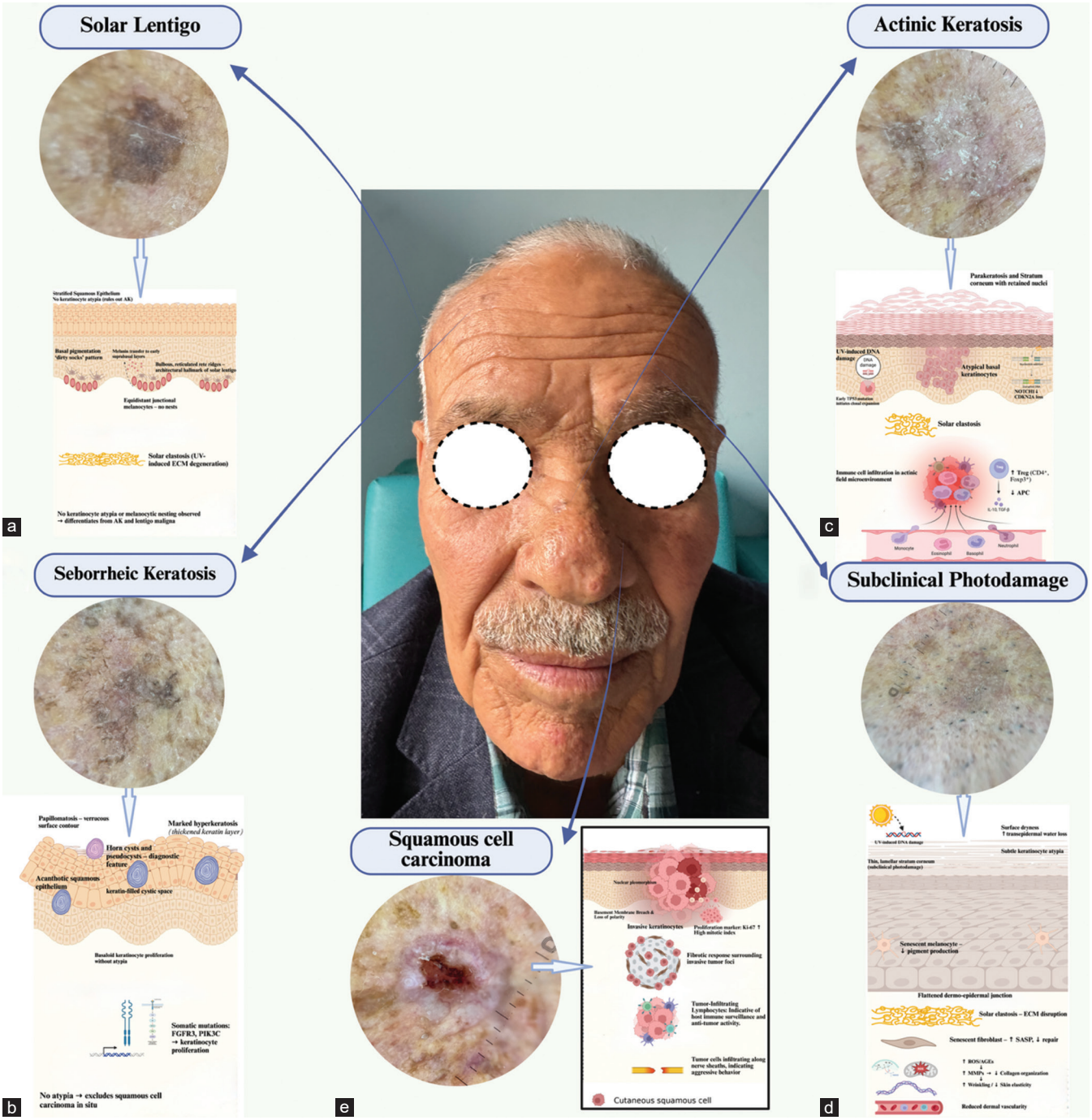
Solar Lentigo
Actinic Keratosis
Seborrheic Keratosis
Subclinical Photodamage
Squamous cell carcinoma
a
b
c
d
e
Basal pigmentation "dirty necks" pattern
Bulbous, reticulated rete ridges – architectural hallmark of solar lentigo
Equidistant junctional melanocytes – no nests
Solar elastosis (UV-induced ECM degeneration)
No keratinocyte atypia or melanocytic nesting observed → differentiates from AK and lentigo maligna
Parakeratosis and Stratum corneum with retained nuclei
UV-induced DNA damage
Atypical basal keratinocytes
Solar elastosis
↑ Treg (CD4⁺, FoxP3⁺)
↓ APC
Papillomatosis – verrucous surface contour
Marked hyperkeratosis (thickened keratin layer)
Horn cysts and pseudocysts – diagnostic feature
Acanthotic squamous epithelium
keratin-filled cystic space
Basaloid keratinocyte proliferation without atypia
Somatic mutations: FGFR3, PIK3C → keratinocyte proliferation
No atypia → excludes squamous cell carcinoma in situ
Surface dryness ↑ transepidermal water loss
Subtle keratinocyte atypia
Senescent melanocyte – ↓ pigment production
Flattened dermo-epidermal junction
Solar elastosis – ECM disruption
Senescent fibroblast – ↑ SASP, ↓ repair
↑ ROS/AGEs
↑ MMPs → ↓ Collagen organization
↑ Wrinkling / ↓ Skin elasticity
Reduced dermal vascularity
Invasive keratinocytes
Proliferation marker: Ki-67 ↑ High mitotic index
Fibrotic response surrounding invasive tumor foci
Tumor-Infiltrating Lymphocytes: Indicative of host immune surveillance and anti-tumor activity.
Tumor cells infiltrating along nerve sheaths, indicating aggressive behavior
Cutaneous squamous cell

Figure 7: Clinicopathologic and dermoscopic correlation of the actinic field spectrum. Composite illustration showing the continuum of UV-induced skin changes in an elderly patient with chronic sun exposure. The central clinical image is accompanied by representative dermoscopic views and schematic histopathology of four distinct conditions: (a) Solar lentigo – benign pigmented lesion with basal pigmentation and rete ridge elongation; (b) Seborrheic keratosis – epidermal hyperplasia with keratin pseudocysts; (c) Actinic keratosis – erythematous, scaly lesion characterized by basal keratinocyte atypia, parakeratosis, and solar elastosis; (d) Subclinical photodamage – clinically inapparent changes with dermoscopic perifollicular granularity and histologic evidence of early UV-induced atypia; and (e) Squamous cell carcinoma – invasive keratinocytic neoplasm representing the malignant endpoint of field cancerization. This figure highlights the clinical, dermoscopic, and histopathological continuum of the actinic field, emphasizing how the TABS–FI framework captures both visible and subclinical disease within this spectrum.

TABS–FI reduces diagnostic ambiguity and provides a standardized measure of premalignant burden.

Phenotypic stratification showed that the moderate FI phenotype was predominant (48%), indicating that intermediate subclinical field involvement represents the typical presentation. Although often underappreciated, this subgroup may still carry a measurable risk of progression to cSCC. Severe field-dominant disease was present in 15% of patients, supporting a proactive, field-

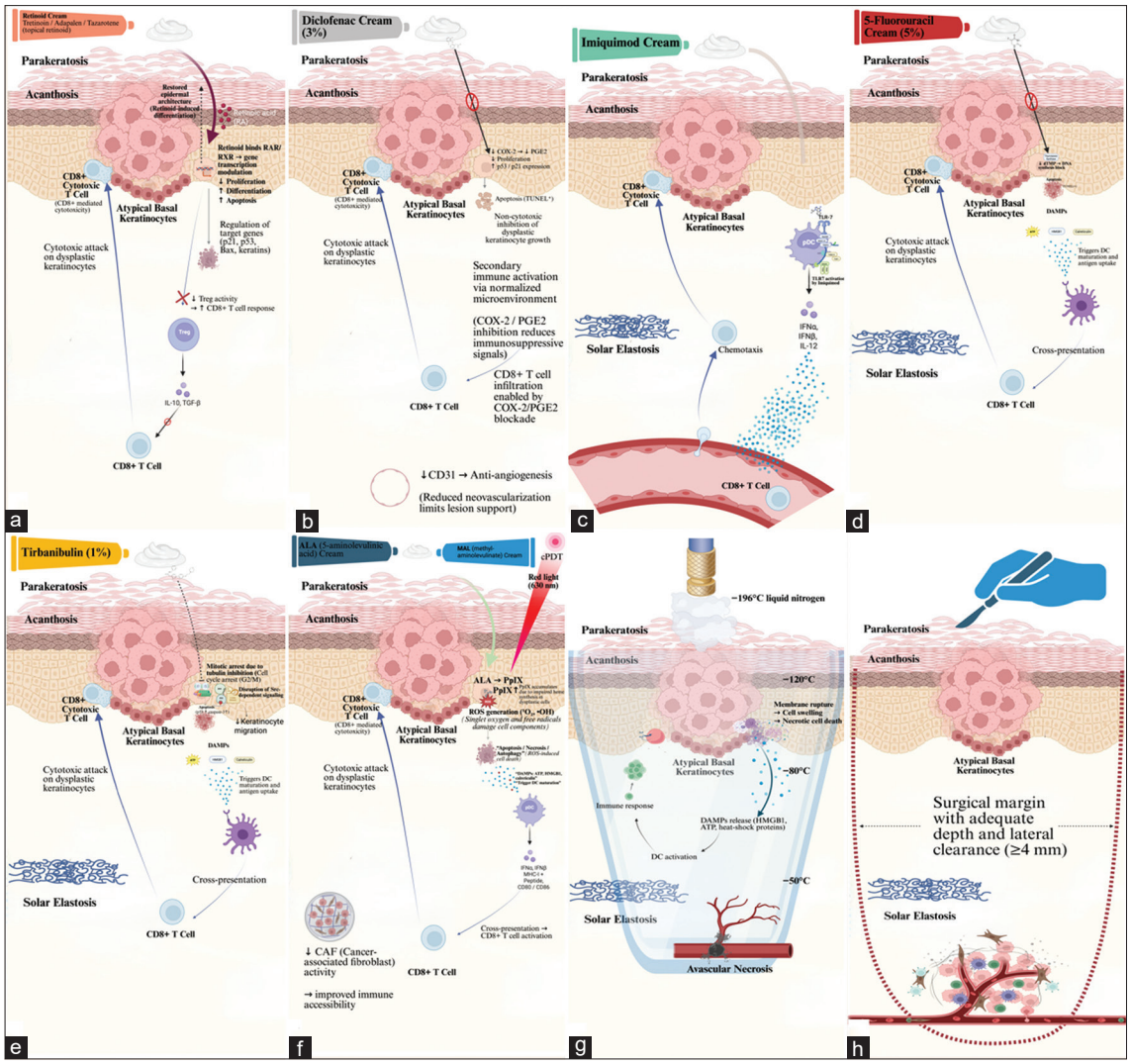

Figure 8: (a-h) Mechanistic overview of therapeutic modalities in actinic keratosis. Schematic representation of eight therapeutic approaches (a–h: topical retinoids, diclofenac, imiquimod, 5-fluorouracil, tirbanibulin, photodynamic therapy, cryotherapy, and excisional biopsy), highlighting their molecular targets, immune interactions, and clinical implications. (Abbreviations: AK, actinic keratosis; COX2, cyclooxygenase-2; TLR-7, toll-like receptor 7; ROS, reactive oxygen species; DAMPs, damage-associated molecular patterns; SPC, superficial perivascular capillary.).

directed approach. Notably, conventional variables—age, occupational UV exposure, and region count—failed to predict severe FI (AUC = 0.46), underscoring the limits of traditional risk tools. In contrast, the TABS tracked lesion number while remaining independent of FI, capturing both visible burden and cumulative photodamage. These observations are concordant with evidence that field therapies such as 5-FU and daylight PDT improve outcomes irrespective of baseline lesion counts [47,48]. Noninvasive imaging, particularly LC-OCT, further demonstrates that actinic damage extends beyond clinical margins [49,50], reinforcing the utility of FI-based stratification (Figure 6).

In our cohort, the TABS–FI system showed a mean FI of 36.2%, with 15% of patients exhibiting severe field-dominant phenotypes, indicating a substantial subclinical burden. These findings are consistent with molecular evidence of Notch pathway dysregulation and elevated NOTCH1 expression in AK, mechanisms that promote a pro-carcinogenic field [51,52]. Complementary imaging studies using ultraviolet-induced fluorescence dermoscopy also demonstrate that subclinical photodamage extends beyond visible margins, reinforcing the clinical value of FI-based stratification for detecting hidden actinic burden [53]. Together, histopathologic, molecular, and imaging data illustrate the continuum from benign photodamage to invasive squamous cell carcinoma, a progression exemplified in Figure 7.

Several indices have been developed to assess AK burden, including AKASI [54,55], AK-FAS [56], total lesion count [44], PAASI [57], MASCK [58], and more recently a composite clinical–dermoscopic–confocal

Table 8: Phenotype-based clinical interpretation of TABS and FI values across the actinic field spectrum†

TABS Range	FI (%) Range	Actinic Field Stage	Clinical Risk Profile	Suggested Management
0–10	<25%	Benign or Subclinical Photodamage (e.g., Seborrheic Keratosis, Lentigo, Early AK)	Minimal damage, very low risk	Observation, photoprotection, annual follow-up
11–17	<25%	Lesion-dominant AK	Localized AK, negligible field damage	Cryotherapy or targeted lesion removal
11–17	25–35%	Subclinical field photodamage	Mild field damage, early actinic field	Lesion therapy+mild field agents (e.g., imiquimod, diclofenac)
11–17	35–45%	Field Cancerization (Moderate field involvement)	Mixed phenotype, progressive risk	PDT or 5-FU+lesion-directed therapy
11–17	>45%	Field-predominant subclinical AK	Moderate TABS, aggressive field involvement	Prioritize full field approach (e.g., topical 5-FU, daylight PDT)
18–24	<35%	Lesion-heavy AK with minor field involvement	High TABS, early field involvement	Lesion excision + close field surveillance
18–24	≥35%	Diffuse Actinic Field Damage	Severe lesion and significant field involvement	Combined field-directed therapies (e.g., topical 5-FU±imiquimod or PDT)
≥25	>45%	Multifocal/Diffuse AK with Prominent Field Involvement	High-risk for cSCC development	Full field therapy + biopsy mapping ± systemic immunomodulators (if indicated, e.g., immunosuppression, recurrent or aggressive lesions)

†This table is intended as a clinical guide rather than a prescriptive algorithm; therapeutic choices should be tailored to guideline recommendations, comorbidities, and patient preferences. (PDT: Photodynamic Therapy; 5-FU: 5-Fluorouracil; AK: Actinic Keratosis; cSCC: Cutaneous Squamous Cell Carcinoma). This table outlines a phenotype-based framework for interpreting TABS and FI scores in actinic keratosis. Patients are stratified into distinct risk categories according to lesion severity and field involvement, supporting individualized therapeutic planning. Lower TABS and FI values correspond to minimal or localized actinic burden, favoring lesion-directed approaches, whereas higher scores indicate extensive field cancerization and the need for comprehensive field-directed therapies. This conceptual stratification facilitates personalized care and dynamic risk assessment in clinical practice.

scoring approach [59]. While each tool provides partial insight, they remain limited by reliance on clinical or photographic features, restricted anatomical scope, and lack of dermoscopic integration for quantifying subclinical field damage. In contrast, the TABS–FI model introduced here integrates lesion- and field-based dermoscopic criteria, enabling stratification into phenotypes such as moderate burden (69%) and severe field-dominant (15%), categories not captured by conventional tools. As summarized in Table 7, TABS–FI combines lesion–field balance, dermoscopic precision, and phenotype-based risk stratification, positioning it as a practical tool for personalized AK management.

Recent literature emphasizes that visible AK lesions represent only the 'tip of the iceberg' of UV-induced dysplasia. In our cohort, mixed-pattern phenotypes were common (41%), and 14% of patients demonstrated severe field-dominant involvement (FI >45%), confirming that substantial subclinical burden may exist even when visible lesion counts are low. This phenotype-based approach underscores the clinical value of TABS–FI and provides a basis for individualized management, consistent with guideline recommendations [60] and recent evidence linking high-risk AK phenotypes with increased cSCC potential [61]. Field-directed therapies such as daylight PDT, 5-FU, and tirbanibulin not only improve clearance but also reduce cSCC risk, as highlighted in updated reviews [62,63]. For patients with severe field damage, adjunctive tools such as RCM may be warranted, supported by systematic evidence for its role in treatment monitoring [64]. Collectively, our findings reinforce the need to move from lesion-centric treatment to dermoscopy-guided, field-integrated strategies [65]. Figure 8 outlines the mechanistic basis of available therapeutic modalities, while Table 8 provides a phenotype-based framework for translating TABS–FI scores into individualized treatment planning.

CONCLUSION

This study introduces the dermoscopy-guided TABS–FI framework to comprehensively quantify both clinical and subclinical actinic keratosis burden. By moving beyond simple lesion counts and incorporating field assessment, the model provides more precise stratification of actinic damage. Our findings demonstrate that substantial subclinical involvement can be present even in patients with few visible lesions. TABS–FI offers a numeric, anatomically adaptable, and reproducible tool that may facilitate personalized management and enhance clinical risk stratification in AK.

IMPLICATIONS FOR FUTURE RESEARCH

Future studies should clarify whether elevated TABS and FI scores predict progression to cSCC, thereby establishing their prognostic value. Validation against histopathological and molecular markers is needed to confirm biological relevance. Interobserver studies are essential to demonstrate reproducibility and clinical reliability. The development of AI-assisted or simplified

scoring platforms could enhance scalability and facilitate integration into routine practice. Finally, longitudinal and multicenter studies across diverse populations and skin phototypes are required to test predictive accuracy and generalizability, supporting the adoption of TABS–FI in daily dermatology and clinical trials.

LIMITATIONS

This study has limitations. It was single-center and relied on a single dermatologist for dermoscopic scoring, so interobserver variability was not assessed. Histopathological confirmation was incomplete, and the TABS–FI framework was validated only internally; multicenter studies are needed to confirm external reproducibility. The system quantifies actinic burden but does not yet predict malignant transformation, and longitudinal data are required to establish prognostic value. Adaptations may also be needed for non-facial sites or darker phototypes. Incorporating advanced imaging modalities such as RCM or LC-OCT could further strengthen diagnostic precision. Despite these constraints, TABS–FI offers a practical, reproducible tool for quantifying actinic damage and guiding personalized management.

ABBREVIATIONS

5-FU: 5-Fluorouracil
AK: Actinic Keratosis
AKASI: Actinic Keratosis Area and Severity Index
AK-FAS: Actinic Keratosis Field Assessment Scale
AUC: Area Under the ROC Curve
BMI: Body Mass Index
CI: Confidence Interval
cSCC: Cutaneous Squamous Cell Carcinoma
COX-2: Cyclooxygenase-2
DAMPs: Damage-Associated Molecular Patterns
DNA: Deoxyribonucleic Acid
dPDT: Daylight Photodynamic Therapy
FI: Field Index
GCP: Good Clinical Practice
IQR: Interquartile Range
IL-10: Interleukin-10
Ki-67: Marker of Cellular Proliferation
LC-OCT: Line-Field Confocal Optical Coherence Tomography
MAPK: Mitogen-Activated Protein Kinase
MASCK: Method for Assessing Skin Cancerization and Keratoses
MMPs: Matrix Metalloproteinases
NF-κB: Nuclear Factor Kappa B
OCT: Optical Coherence Tomography
OR: Odds Ratio
PAASI: Photoaging Area and Severity Index
PDT: Photodynamic Therapy
PGA: Physician Global Assessment
PI3K/AKT/mTOR: Phosphoinositide-3-Kinase/Protein Kinase B/Mammalian Target of Rapamycin pathway
RCM: Reflectance Confocal Microscopy
ROC: Receiver Operating Characteristic
ROS: Reactive Oxygen Species
SD: Standard Deviation
SOD: Superoxide Dismutase
SPC: Superficial Perivascular Capillary
TABS: Total Actinic Keratosis Burden Score
TGF-β: Transforming Growth Factor Beta
TLC: Total Lesion Count
TLR-7: Toll-Like Receptor 7
TP53: Tumor Protein p53
UV: Ultraviolet

REFERENCES

1. Marques E, Chen TM. Actinic keratosis. StatPearls Publishing; 2023.
2. Fargnoli MC, Altomare G, Benati E, Casari A, Schmitz L, Gupta G, et al. Prevalence and risk factors of actinic keratosis in patients attending Italian dermatology clinics. Eur J Dermatol. 2017;27:599–608.
3. George CD, Lee T, Hollestein LM, Asgari MM, Nijsten T. Global epidemiology of actinic keratosis in the general population: a systematic review and meta-analysis. Br J Dermatol. 2024;190:465–76.
4. Noels EC, Hollestein LM, van Egmond S, Lugtenberg M, van Nistelrooij LPJ, Bindels PJE, et al. Healthcare utilization and management of actinic keratosis in primary and secondary care. Br J Dermatol. 2019;181:544–53.
5. Balcere A, Konrade-Jilmaza L, Paulina LA, Cema I, Krumina A. Clinical characteristics of actinic keratosis associated with progression risk. J Clin Med. 2022;11:5899.
6. Werner RN, Sammain A, Erdmann R, Hartmann V, Stockfleth E, Nast A, et al. The natural history of actinic keratosis: a systematic review. Br J Dermatol. 2013;169:502–18.
7. Cribier B. Clinicopathologic diagnosis of actinic keratosis. Ann Dermatol Venereol. 2019;146 Suppl 2:IIS10–IIS15.
8. Conforti C, Ambrosio L, Retrosi C, Cantisani C, Di Lella G, Fania L, et al. Clinical and dermoscopic diagnosis of actinic keratosis. Dermatol Pract Concept. 2024;14:e2024147S.
9. Soare C, Cozma EC, Celarel AM, Rosca AM, Lupu M, Voiculescu VM, et al. Digitally enhanced methods for the diagnosis of actinic keratoses. Cancers (Basel). 2024;16:484.
10. Slaughter DP, Southwick HW, Smejkal W. Field cancerization in oral stratified squamous epithelium. Cancer. 1953;6:963–8.
11. Jetter N, Chandan N, Wang S, Tsoukas M. Field cancerization therapies for actinic keratosis. Am J Clin Dermatol. 2018;19:543–57.
12. Isik B, Gurel MS, Erdemir AT, Kesmezacar O. Development of skin aging scale using dermoscopy. Skin Res Technol. 2013;19:69–74.
13. Zhao J, Zhang X, Tang Q, Bi Y, Yuan L, Yang B, et al. Correlation between dermoscopy and clinical and pathological findings in photoaging. Skin Res Technol. 2024;30:e13578.
14. Gilchrest BA. Actinic keratoses: biology and treatment paradigms. J Invest Dermatol. 2021;141:727–31.

15. Philipp-Dormston WG. Field cancerization. In: Soyer HP, Prow TW, Jemec GBE, editors. Actinic keratosis. Basel: Karger; 2014. p.115–21.
16. Wei J, Kok LF, Byrne SN, Halliday GM. Photodamage and early SCC. In: Soyer HP, Prow TW, Jemec GBE, editors. Actinic keratosis. Basel: Karger; 2014. p.14–19.
17. Burstein SE, Maibach H. Actinic keratosis metrics. Arch Dermatol Res. 2024;316:543.
18. Philipp-Dormston WG, Sanclemente G, Torezan L, Tretti Clementoni M, Le Pillouer-Prost A, Cartier H, et al. Daylight photodynamic therapy for photodamaged skin. J Eur Acad Dermatol Venereol. 2016;30:8–15.
19. Szeimies RM, Atanasov P, Bissonnette R. Use of lesion response rate in actinic keratosis trials. Dermatol Ther. 2016;6:461–64.
20. Kopera D, Torrano J, Soyer HP. Treating subclinical actinic keratosis. JEADV Clin Pract. 2023;2:786–91.
21. Acar A, Karaarslan I. Comparison of actinic keratosis indices with PGA and TLC. Dermatol Pract Concept. 2022;12:e2022031.
22. Schmitz L, Kahl P, Majores M, Bierhoff E, Stockfleth E, Dirschka T, et al. Correlation between clinical and histological classification systems in AK. J Eur Acad Dermatol Venereol. 2016;30:1303–7.
23. Ahmady S, Jansen MHE, Nelemans PJ, Kessels JPHM, Arits AHMM, de Rooij MJM, et al. Risk of invasive cSCC after AK treatments. JAMA Dermatol. 2022;158:634–40.
24. Schmitz L, Gambichler T, Gupta G, Stucker M, Dirschka T, et al. AKASI and risk of squamous cell carcinoma. J Eur Acad Dermatol Venereol. 2018;32:752–6.
25. Kim YS, Shin S, Jung SH, Park YM, Park GS, Lee SH, et al. Genomic progression from AK to SCC. J Invest Dermatol. 2022;142:528–38.
26. Li Z, Lu F, Zhou F, Song D, Chang L, Liu W, et al. From AK to cSCC: pathogenesis and treatments. Front Immunol. 2025;16:1518633.
27. Wang Z, Wang X, Shi Y, Wu S, Ding Y, Yao G, et al. Advances in AK pathogenesis. Front Med. 2024;11:1330491.
28. Worley B, Harikumar V, Reynolds K, Dirr MA, Christensen RE, Anvery N, et al. Treatment of actinic keratosis: systematic review. Arch Dermatol Res. 2023;315:1099–108.
29. Malvehy J, Stratigos AJ, Bagot M, Stockfleth E, Ezzedine K, Delarue A, et al. Actinic keratosis: current challenges. J Eur Acad Dermatol Venereol. 2024;38:1481–92.
30. Del Regno L, Catapano S, Di Stefani A, Cappilli S, Peris K. Therapies for actinic keratosis. Am J Clin Dermatol. 2022;23:339–52.
31. Del Marmol V. Euromelanoma campaign: 20 years. J Eur Acad Dermatol Venereol. 2022;36 Suppl 6:5–11.
32. Karp P, Karp K, Kadziela M, Zajdel R, Zebrowska A, et al. Early detection of atypical skin lesions. Cancers (Basel). 2024;16:4264.
33. D'Onghia M, Falcinelli F, Barbarossa L, Pinto A, Cartocci A, Tognetti L, et al. Zoom-in dermoscopy for facial tumors. Diagnostics (Basel). 2025;15:324.
34. Respati RA, Yusharyahya SN, Wibawa LP, Widaty S. Dermoscopic features of photoaging. Clin Cosmet Investig Dermatol. 2022;15:939–46.
35. Thamm JR, Schuh S, Welzel J. Epidemiology and risk factors of AK. Dermatol Pract Concept. 2024;14:e2024146S.
36. Cramer P, Stockfleth E. Future of actinic keratosis management. Expert Opin Emerg Drugs. 2020;25:49–58.
37. Soare C, Cozma EC, Porosnicu AL, Cristian DA, Mandi DM, Giurcaneanu C, et al. Clinico-pathologic profile of AK patients. Cancers (Basel). 2025;17:1923.
38. John SM, Trakatelli M, Gehring R, Finlay K, Fionda C, Wittlich M, et al. Non-melanoma skin cancer as occupational disease. J Eur Acad Dermatol Venereol. 2016;30 Suppl 3:38–45.
39. Woodie BR, Jones G, Holovach P, Fleischer AB Jr. Sex differences in AK distribution. Arch Dermatol Res. 2025;317:526.
40. Fartasch M, Diepgen TL, Schmitt J, Drexler H. Occupational sun exposure and skin cancer. Dtsch Arztebl Int. 2012;109:715–20.
41. Stockfleth E, Begeault N, Delarue A. AK lesion count vs total burden. Curr Ther Res Clin Exp. 2021;96:100661.
42. Figueras Nart I, Cerio R, Dirschka T, Dreno B, Lear JT, Pellacani G, et al. Defining actinic field. J Eur Acad Dermatol Venereol. 2018;32:544–63.
43. Heppt MV, Leiter U, Steeb T, Amaral T, Bauer A, Becker JC, et al. S3 guideline for AK and cSCC. J Dtsch Dermatol Ges. 2020;18:275–94.
44. McCampbell L, Zaino M, Prajapati S, Kontzias C, Feldman SR. AK number vs field size. J Cutan Med Surg. 2023;27:664–5.
45. Chung HJ, McGuigan KL, Osley KL, Zendell K, Lee JB. Pigmented AK. J Am Acad Dermatol. 2013;68:647–53.
46. Akay BN, Kocyigit P, Heper AO, Erdem C. Dermoscopy of pigmented facial lesions. Br J Dermatol. 2010;163:1212–7.
47. Weinstock MA, Thwin SS, Siegel JA, Marcolivio K, Means AD, Leader NF, et al. Chemoprevention with 5-FU. JAMA Dermatol. 2018;154:167–74.
48. Wiegell SR, Fredman G, Andersen F, Bjerring P, Paasch U, Haedersdal M, et al. 5-FU and daylight PDT trial. Photodiagnosis Photodyn Ther. 2024;46:104069.
49. Cinotti E, Tognetti L, Cartocci A, Lamberti A, Gherbassi S, Orte Cano C, et al. LC-OCT in AK and SCC. Clin Exp Dermatol. 2021;46:1530–41.
50. Razi S, Kuo YH, Pathak G, Agarwal P, Horgan A, Parikh P, et al. LC-OCT meta-analysis. Diagnostics (Basel). 2024;14:1522.
51. Shi Q, Xue C, Zeng Y, Yuan X, Chu Q, Jiang S, et al. Notch signaling in cancer. Signal Transduct Target Ther. 2024;9:128.
52. Li Z, Lu F, Zhou F, Song D, Chang L, Liu W, et al. AK to SCC progression. Front Immunol. 2025;16:1518633.
53. Korecka K, Polanska A, Danczak-Pazdrowska A, Navarrete-Dechent C. UV fluorescence dermoscopy in AK. Photodiagnosis Photodyn Ther. 2024;46:104056.
54. Dirschka T, Pellacani G, Micali G, Malvehy J, Stratigos AJ, Casari A, et al. AKASI scoring system. J Eur Acad Dermatol Venereol. 2017;31:1295–302.
55. Pellacani G, Gupta G, Micali G, Malvehy J, Stratigos AJ, Casari A, et al. AKASI reproducibility study. Br J Dermatol. 2018;179:763–4.
56. Dreno B, Cerio R, Dirschka T, Nart IF, Lear JT, Peris K, et al. AK-FAS scale. Acta Derm Venereol. 2017;97:1108–13.
57. Nevakivi R, Siiskonen H, Haimakainen S, Harvima IT. Skin lesion spectrum study. BMC Cancer. 2024;24:338.
58. Baker C, James A, Supranowicz M, Spelman L, Shumack S, Cole J, et al. MASCK development study. Clin Exp Dermatol. 2022;47:1144–53.
59. Soare C, Cozma EC, Giurcaneanu C, Voiculescu VM. Composite scoring of AK. Cancers (Basel). 2025;17:2899.
60. Eisen DB, Asgari MM, Bennett DD, Connolly SM, Dellavalle RP, Freeman EE, et al. Guidelines of care for AK. J Am Acad Dermatol. 2021;85:e209–33.
61. Knuutila JS, Kaijala O, Lehto S, Vahlberg T, Nissinen L, Kahari VM, et al. Risk factors for cSCC in AK patients. Acta Derm Venereol. 2024;104:adv40990.
62. Aggarwal I, Puyana C, Chandan N, Jetter N, Tsoukas M. Field therapies update. Am J Clin Dermatol. 2024;25:391–405.
63. Paradisi A, Bocchino E, Mannino M, Gualdi G, D'Amore A, Traini DO, et al. Treatment of AK and field cancerization. J Pers Med. 2025;15:421.
64. Zhang J, Ran H, Zhao Y, Liang X, Gu Z, Xue Y, et al. RCM in AK monitoring. Photodiagnosis Photodyn Ther. 2025;53:104539.
65. Kandolf L, Peris K, Malvehy J, Mosterd K, Heppt MV, Fargnoli MC, et al. European consensus guideline for AK. J Eur Acad Dermatol Venereol. 2024;38:1024–47.

Copyright by Gökhan Kaya. This is an open-access article distributed under the terms of the Creative Commons Attribution License, which permits unrestricted use, distribution, and reproduction in any medium, provided the original author and source are credited.

Source of Support: This article has no funding source.

Conflict of Interest: The authors have no conflict of interest to declare.